Article

Effects of Zr Addition on Thermodynamic and Kinetic Properties of Liquid Mg-6Zn-*x*Zr Alloys

Ye Yuan [1,2], **Yuan Huang** [1,*] **and Qiang Wei** [2,*]

1   Institute of Advanced Metallic Materials, School of Material Science and Engineering, Tianjin University, Tianjin 300072, China; yuanye132764@tju.edu.cn
2   School of Mechanical Engineering, Hebei University of Technology, Tianjin 300130, China
*   Correspondence: yi_huangyuan@tju.edu.cn (Y.H.); weiqiang@tju.edu.cn (Q.W.);
    Tel.: +86-1392-083-8071 (Y.H.); +86-1321-207-7725 (Q.W.)

check for updates

Abstract: Mg-6Zn-*x*Zr (ZK60) alloys are precipitation strengthened by Mg-Zn intermetallics. Therefore, it is important to investigate the thermodynamic and kinetic effects of Zr addition on formations of these reinforcement phases (Mg_7Zn_3, $MgZn_2$, and MgZn) in Mg-6Zn-*x*Zr melts. Because it is difficult to gain thermodynamic and kinetic data in melts by experiment, obtaining these data points still depends on a theoretical calculation. Based on the Miedema formation enthalpy model and the Chou model, the thermodynamic properties (the mixing enthalpies, the Gibbs free energies, and the component activities) of Mg-6Zn-*x*Zr ternary alloys and their constitutive binary alloys are calculated. The thermodynamic effects of Zr addition on formations of Mg_7Zn_3, $MgZn_2$, and MgZn are predicted. Using a ternary model for predicting diffusion coefficients, the diffusion coefficients of Zn and Zr in liquid Mg-6Zn-*x*Zr alloys are calculated and the kinetic effects of Zr addition on the diffusion coefficient of Zn is discussed. The results show that the Zr addition can hinder the formations of Mg_7Zn_3, $MgZn_2$, and MgZn inter-metallics in thermodynamics and kinetics.

Keywords: Mg-6Zn-*x*Zr alloy; zirconium; Mg-Zn intermetallic compounds; thermodynamics; kinetics; Miedema model; diffusion coefficient

1. Introduction

Magnesium alloys have great potential applications in aerospace and automotive industries [1] because of their low density, high specific strength, and good castability [2,3]. Currently, the world annual production of magnesium is in the third place, just behind steel and aluminum [4]. Mg-Zn based alloys are one of the most important commercial magnesium alloys. However, Mg-Zn binary alloys are rarely used alone as cast or deformed magnesium alloys due to their coarse crystal grain [5]. Therefore, Zr, as a powerful grain refiner of magnesium alloys, is usually added to the Mg-Zn alloy to improve its strength and plasticity [6]. Now, the Mg-Zn-Zr (ZK) alloys have been widely used in industry due to its high specific strength and improved plasticity. Because the maximum solubility of zirconium in liquid magnesium is below 0.6 wt% and the corrosion resistance of Mg-Zn-Zr alloys will decrease when the Zn content exceeds 6 wt%. We aimed to investigate the effects of Zr addition on thermodynamic and kinetic properties in Mg-Zn-Zr melts. Therefore, the Zn content is fixed at 6 wt% and the Zr content varies from 0 wt% to 0.6 wt%, and then the thermodynamic and kinetic effects of Zr addition on thermodynamic and kinetic properties in Mg-6Zn-*x*Zr (*x* = 0–0.6 wt%) ternary alloys are discussed.

In Mg-6Zn-*x*Zr (*x* = 0–6 wt%) alloys, it has been reported that the main strengthening phase are Mg_7Zn_3, $MgZn_2$, and MgZn [7,8]. These reinforcement phases precipitate in the melt by chemical reactions between elements [9]. The effects of Zr additions on these reactions in the melt have not been further studied. To date, the investigations have been mainly focused on the type and content of

precipitate phases in the cast Mg-6Zn-*x*Zr alloys (x = 0–6 wt%) by changing the Zr composition and technical processes (time and temperature) [7,8]. However, theoretical research studies on the effect of Zr addition on the formation of Mg_7Zn_3, $MgZn_2$, and MgZn compounds in Mg-6Zn-*x*Zr alloys (x = 0–6 wt%) are rather few.

It is widely recognized that the formation of the precipitated phase in melts are controlled by the thermodynamics and kinetics of alloy systems [10,11]. The alloy addition can play a key role in influencing the thermodynamic and kinetic properties of alloy systems and, hence, effect the formation of the precipitated phase in melts. Thermodynamically, the alloy addition can influence the Gibbs free energies of precipitated compounds by changing the component activities in melts, and consequently influence the nucleation of these strengthening phases. Kinetically, the alloy addition can influence the diffusion rates of components by changing the mutual diffusion coefficients in melts, and consequently influence the growth of precipitated compounds. However, little research emphasizes the effect of Zr addition on the thermodynamic and kinetic properties of liquid Mg-6Zn-*x*Zr alloys (x = 0–6 wt%).

Therefore, the effect of Zr addition on the liquid Mg-6Zn-*x*Zr (x = 0–6 wt%) ternary alloys should be investigated in thermodynamics and kinetics. However, the thermodynamic and kinetic data are rather scarce in Mg-6Zn-*x*Zr (x = 0–6 wt%) ternary systems because of the experimental difficulties. Therefore, it is necessary to calculate the thermodynamic and kinetic data for liquid Mg-6Zn-*x*Zr (x = 0–6 wt%) alloys according to some established theory models.

Using the component activities, the Gibbs free energies can be theoretically calculated by some thermodynamic models. The Miedema model [12] and Chou model [13–15] have been established for the thermodynamic calculation of alloy systems. Therefore, these models are used to calculate the thermodynamic properties (the mixing enthalpies, the component activities, and the Gibbs free energies) of liquid Mg-6Zn-*x*Zr (x = 0–6 wt%) alloys in this work.

In order to obtain the mutual diffusion coefficients in melts, a prediction model is needed. Kirkaldy [16] has studied the relationship between the mutual diffusion coefficient and intrinsic diffusion coefficient for a ternary system and pointed out that the intrinsic diffusion coefficient can be calculated from the thermodynamic factors and the self-diffusion coefficient of each component. The thermodynamic factor is related to the component activity that can be predicted by the previously mentioned thermodynamic models. Meanwhile, the self-diffusion coefficient of each component can be predicted based on the hard sphere theory, which is the most widely used approach [17]. Base on Kirkaldy's works and the hard sphere theory, Ding [18] presented a kinetic prediction model for mutual diffusion coefficients, according to the thermodynamic factors, and the self-diffusion coefficients of components in a ternary alloy. In addition, the self-diffusion coefficient of each component can be obtained by Schwitzgebel's model [19], which has been successfully applied to predict the interdiffusion coefficients in the ternary system [18]. In this paper, the above prediction models are used to obtain the interdiffusion coefficients in liquid Mg-6Zn-*x*Zr (x = 0–0.6 wt%) alloys.

Based on the above calculation results, the thermodynamic and kinetic effects of Zr addition on the formation mechanism of the precipitated phase (Mg_7Zn_3, $MgZn_2$, and MgZn) in liquid Mg-6Zn-*x*Zr (x = 0–6 wt%) alloys can be discussed. The final results in this paper show that Zr addition can hinder the precipitation of Mg_7Zn_3, $MgZn_2$, and MgZn thermodynamically and kinetically.

2. Calculation Model

2.1. Miedema Model and Chou Model for Thermodynamic Calculation of Mg-Zn-Zr Alloys

The Miedema model is a semi-empirical model, which can be used to predict the thermodynamic properties of binary alloys. Extrapolated from the Miedema model, the Chou model was established to calculate the thermodynamic properties of ternary alloys [13–15]. In order to obtain the thermodynamic parameters of Mg-Zn-Zr system, it first needs to calculate the thermodynamic parameters of its three constitutive binary systems (Mg-Zn, Mg-Zr, and Zr-Zn binary systems) by the Miedema model.

For an *i-j* disordered solution, the enthalpy of mixing can be calculated by the Miedema model as follows [20].

$$\Delta H_{ij} = f_{ij} \times \frac{x_i[1 + u_i x_j(\phi_i^* - \phi_j^*)]x_j[1 + u_j x_i(\phi_i^* - \phi_j^*)]}{x_i V_i^{2/3}[1 + u_i x_j(\phi_i^* - \phi_j^*)] + x_j V_j^{2/3}[1 + u_j x_i(\phi_i^* - \phi_j^*)]} \tag{1}$$

For a binary ordered stoichiometric compound, the enthalpy of formation can be expressed using the equation below [12].

$$\Delta H_{ij}^{\text{order}} = \Delta H_{ij}\left[1 + \gamma \times \left(\frac{\Delta H_{ij}}{f_{ij} \times \left\{x_i V_i^{2/3}[1 + u_i x_j(\phi_i^* - \phi_j^*)] + x_j V_j^{2/3}[1 + u_j x_i(\phi_i^* - \phi_j^*)]\right\}}\right)^2\right] \tag{2}$$

In which

$$f_{ij} = \frac{2PV_i^{2/3}V_j^{2/3}\left[-(\phi_i^* - \phi_j^*)^2 + \frac{Q}{P}(n_{\text{ws}_i}^{1/3} - n_{\text{ws}_j}^{1/3})^2 - \alpha\frac{R}{P}\right]}{(n_{\text{ws}_i})^{-1/3} + (n_{\text{ws}_j})^{-1/3}} \tag{3}$$

where *i* and *j* are the two components in a binary alloy system, n_{WS} is the electron density, ϕ^* is the electronegativity, V_i is the mole volume of *i* atom, and x_i and x_j are the mole fractions of components *i* and *j*, respectively. *R*, *Q*, *P*, *u*, and α are all empirical parameters. The *R/P* term exists only when a transition metal is alloyed with a non-transition metal. The *Q/P* ratio is maintained at 9.4, but the value of *P* is different for different alloy systems [12]. *u* is a constant, which depends on element valence. The factor α takes the values of 0.73 and 1 for liquid alloys and solid alloys, respectively [12]. These physical and empirical parameters can be obtained from Tables 1–3.

Table 1. The parameters of Mg, Y, Zn, and Zr, data from [12].

Element	$T_{\mathbf{m}}$	$\phi^*(V)$	$n_{ws}^{1/3}$	$V^{2/3}(\text{cm}^2)$	u
Mg	923	3.45	1.17	5.81	0.10
Zn	693	4.10	1.32	4.38	0.10
Zr	2125	3.45	1.41	5.81	0.07

Table 2. The R/P parameter of Mg, Y, Zn, and Zr, data from [12].

Metal	Transition Metal		Non-Transition Metal	
Element	Y	Zr	Mg	Zn
R/P	0.7	1.0	0.4	1.4

Table 3. The parameters of alloy system, data from [12].

Alloy	P	R/P
Transition—Transition	14.1	0
Transition—Non-transition	12.3	$(R/P)_i \cdot (R/P)_j$
Non-transition—Non-transition	10.6	0

For a binary alloy, the relationships of mixing enthalpies, excess Gibbs free energies, and excess entropies can be expressed as:

$$G_{ij}^{\text{E}} = \Delta H_{ij} - TS_{ij}^{\text{E}} \tag{4}$$

where *T* represents the absolute temperature of the liquid melt, and S_{ij}^{E} is the excess entropy, which can be calculated as follows [21].

$$S_{ij}^{\text{E}} = 0.1 \times \Delta H_{ij}\left(\frac{1}{T_{mi}} + \frac{1}{T_{mj}}\right) \tag{5}$$

where T_{mi} and T_{mj} are the melting points of components i and j, respectively.

According to the Chou model [12,15], as extrapolated from constitutive binary systems, the thermodynamic parameters (ΔH_{ij}, G_{ij}^{E}, and S_{ij}^{E}) in a ternary system can all be calculated by the following equation.

$$Z_{ijk} = \frac{x_i x_j Z_{ij}(X_i, X_j)}{X_{i(ij)} X_{j(ij)}} + \frac{x_i x_k Z_{ik}(X_i, X_k)}{X_{i(ik)} X_{k(ik)}} + \frac{x_j x_k Z_{jk}(X_j, X_k)}{X_{j(jk)} X_{k(jk)}} \tag{6}$$

where Z_{ijk} is referred to the thermodynamic properties (ΔH_{ij}, G_{ij}^{E}, S_{ij}^{E}) of a ternary alloy, and Z_{ij}, Z_{jk}, and Z_{ik} represent the thermodynamic properties (ΔH_{ij}, G_{ij}^{E}, S_{ij}^{E}) of *i-j*, *j-k*, and *i-k* binary alloys, respectively. Additionally, *i*, *j*, and *k* in Equation (6) are the three components in a ternary alloy system, and x_i, x_j, and x_k are the mole fractions of components *i*, *j*, and *k*, respectively. Lastly, $X_{i(ij)}$ and $X_{j(ij)}$ in Equation (6) are the mole fractions of components *i* and *j* in the selected binary system *i-j* from the ternary system. These parameters of constitutive binary systems can be obtained by using the following formulas.

$$\left. \begin{array}{ll} X_{i(ij)} = x_i + \xi_{ij} x_k & X_{j(ij)} = x_j + \xi_{ji} x_k \\ X_{i(ik)} = x_i + \xi_{ik} x_j & X_{k(ik)} = x_k + \xi_{ki} x_j \\ X_{j(jk)} = x_j + \xi_{jk} x_i & X_{k(jk)} = x_k + \xi_{kj} x_i \end{array} \right\} \tag{7}$$

with

$$\left. \begin{array}{ll} \xi_{ij} = \frac{\eta_i}{\eta_i + \eta_j} & \xi_{ji} = \frac{\eta_j}{\eta_i + \eta_j} \\ \xi_{jk} = \frac{\eta_j}{\eta_k + \eta_j} & \xi_{kj} = \frac{\eta_k}{\eta_k + \eta_j} \\ \xi_{ki} = \frac{\eta_k}{\eta_k + \eta_i} & \xi_{ik} = \frac{\eta_i}{\eta_k + \eta_i} \end{array} \right\} \tag{8}$$

and

$$\left. \begin{array}{l} \eta_i = \int_0^1 \left(G_{ij}^{\mathrm{E}} - G_{ki}^{\mathrm{E}} \right)^2 dX_i \\ \eta_j = \int_0^1 \left(G_{jk}^{\mathrm{E}} - G_{ij}^{\mathrm{E}} \right)^2 dX_j \\ \eta_k = \int_0^1 \left(G_{ki}^{\mathrm{E}} - G_{jk}^{\mathrm{E}} \right)^2 dX_k \end{array} \right\} \tag{9}$$

where η_i, η_j, and η_k represent the deviation functions. The deviation function expression is not unique [14]. There are plenty of expressions to fulfill the requirements for the model [14,15]. In this part, we choose a widely-used one that can reflect the difference between binary systems in the whole composition range through integral. ξ_{ij} in Equations (6) and (7) is the similarity coefficient that ranges from 0 to 1. A small similarity coefficient value means that component *k* is similar to *j*, and a large value means that component *k* is similar to *i* [14]. The ξ_{ij} value can represent the similarity of component *k* to *i* or *j*.

Zr addition can influence the Gibbs free energy of Mg-Zn compounds, and, consequently, influence the nucleation of the corresponding strengthening phases. In Mg-6Zn-*x*Zr ($x = 0$–6 wt%) alloys, the main strengthening phase (e.g., Mg_7Zn_3, $MgZn_2$, and $MgZn$) [7,8,22,23] can be formed through these reactions.

$$7[\mathrm{Mg}] + 3[\mathrm{Zn}] = Mg_7Zn_3(\mathrm{s}) \tag{10}$$

$$[\mathrm{Mg}] + 2[\mathrm{Zn}] = MgZn_2(\mathrm{s}) \tag{11}$$

$$[\mathrm{Mg}] + [\mathrm{Zn}] = MgZn(\mathrm{s}) \tag{12}$$

Via Equations (10)–(12), the Gibbs free energy associated with the formation of Mg-Zn compounds can be calculated by using the formulas below.

$$\Delta G_{\mathrm{Mg_7Zn_3}} = \Delta G_{\mathrm{Mg_7Zn_3}}^{\theta} - RT \ln a^7([\mathrm{Mg}]) a^3([\mathrm{Zn}]) \tag{13}$$

$$\Delta G_{\mathrm{MgZn_2}} = \Delta G_{\mathrm{MgZn_2}}^{\theta} - RT \ln a([\mathrm{Mg}])a^2([\mathrm{Zn}]) \tag{14}$$

$$\Delta G_{\mathrm{MgZn}} = \Delta G_{\mathrm{MgZn}}^{\theta} - RT \ln a([\mathrm{Mg}])a([\mathrm{Zn}]) \tag{15}$$

where $\Delta G_{\mathrm{Mg_7Zn_3}}$, $\Delta G_{\mathrm{MgZn_2}}$, and ΔG_{MgZn} are the Gibbs free energy of formation of $\mathrm{Mg_7Zn_3}$, $\mathrm{MgZn_2}$, and MgZn compounds, respectively. The smaller the Gibbs free energy of formation of a compound, the larger the formation tendency of a compound is. $\Delta G_{\mathrm{Mg_7Zn_3}}^{\theta}$, $\Delta G_{\mathrm{MgZn_2}}^{\theta}$, and $\Delta G_{\mathrm{MgZn}}^{\theta}$ in Equations (13)–(15) are the standard Gibbs free energies of formation of $\mathrm{Mg_7Zn_3}$, $\mathrm{MgZn_2}$, and MgZn, respectively. According to the previous investigation reported by Lun et al. [24], these standard Gibbs free energies can be obtained. For the liquid ternary Mg-6Zn-xZr (x = 0–0.6 wt%) alloys, $a([\mathrm{Zn}])$, $a([\mathrm{Mg}])$ and $a([\mathrm{Zr}])$ in Equations (13)–(15) represent the activities of Zn, Mg, and Zr, respectively, in the liquid ternary alloys. Based on the Miedema model [19] and the Chou model [13,15], the activity of the component *i* can be expressed using Equation (16) below.

$$\alpha_i = \gamma_i \cdot x_i \tag{16}$$

where γ_i is the activity coefficient and x_i is the mole fraction of component *i*. The activity coefficient γ_i is defined as follows [13,15,18].

$$RT \ln \gamma_i = \overline{G_i}^E \tag{17}$$

where *R* is the mole gas constant, *T* is the absolute temperature of the alloy, and $\overline{G_i}^E$ is the partial excess free energy of component *i*.

In a binary alloy, the relationship between $\overline{G_i}^E$ and G_{ij}^E (see Equation (4)) is given by the equation below.

$$\overline{G_i}^E = G_{ij}^E + (1 - x_i)\frac{\partial G_{ij}^E}{\partial x_i} \tag{18}$$

In the *i-j-k* ternary alloy system with *k* as the solvent, the relationship between the partial mole free energy of a component ($\overline{G_i}^E$) and the mole free energy of the ternary system (G_{ijk}^E) is given by Equation (19) below [25].

$$\left.\begin{array}{l} \overline{G_i}^E = G_{ijk}^E - x_j \dfrac{\partial G_{ijk}^E}{\partial x_j} + (1 - x_i)\dfrac{\partial G_{ijk}^E}{\partial x_i} \\[2mm] \overline{G_j}^E = G_{ijk}^E - x_i \dfrac{\partial G_{ijk}^E}{\partial x_i} + (1 - x_j)\dfrac{\partial G_{ijk}^E}{\partial x_j} \\[2mm] \overline{G_k}^E = G_{ijk}^E - x_i \dfrac{\partial G_{ijk}^E}{\partial x_i} - x_j \dfrac{\partial G_{ijk}^E}{\partial x_j} \end{array}\right\} \tag{19}$$

According to Equations (16)–(19), the activity of component *i* in binary or ternary alloys can be obtained by the following equation.

$$\alpha_i = x_i \exp(\overline{G_i}^E / RT) \tag{20}$$

2.2. Diffusion Coefficients Model for Calculation of Kinetic Properties of the Mg-6Zn-xZr Alloy

The diffusion rates of Zn and Zr can be determined by the mutual diffusion coefficients in the Mg-6Zn-xZr (x = 0–6 wt%) melt. According to Ding's prediction model of diffusion coefficients for ternary alloys [16,18], diffusion in a ternary system can be fully expressed by the four interdiffusion coefficients (D_{ii}, D_{jj}, D_{ij}, and D_{ji}). The interdiffusion coefficients are expressed as the following functions of the intrinsic diffusion coefficients and the mole fractions of components (in this paper, where *i*, *j*, and *k* represent components Zn, Zr, and Mg, respectively) [16,18].

$$\left\{\begin{array}{l} D_{ii} = D_{ii}^k - x_i(D_{ii}^k + D_{ji}^k + D_{ki}^k) \\[1mm] D_{ij} = D_{ij}^k - x_i(D_{ij}^k + D_{jj}^k + D_{kj}^k) \\[1mm] D_{ji} = D_{ji}^k - x_j(D_{ii}^k + D_{ji}^k + D_{ki}^k) \\[1mm] D_{jj} = D_{jj}^k - x_j(D_{ij}^k + D_{jj}^k + D_{kj}^k) \end{array}\right. \tag{21}$$

where D_{ii} and D_{jj} refer to the main interdiffusion coefficients, and D_{ij} and D_{ji} are cross interdiffusion coefficients. The main interdiffusion coefficients D_{ii} and D_{jj} represent the influence of the concentration gradients of components i and j on their own fluxes. The cross interdiffusion coefficients D_{ij} and D_{ji} represent the influence of concentration gradients of components j and i on the other fluxes of i and j [16,18], respectively. D_{ii}^k, D_{jj}^k, D_{ik}^k, D_{ki}^k, D_{ji}^k, and D_{ij}^k are the intrinsic diffusion coefficients, which can be expressed as the following functions of the self-diffusion coefficients and thermodynamic interaction coefficients [16,18].

$$D_{ii}^k = \frac{x_i D_{ii}^*}{RT} \cdot \frac{\partial \mu_i}{\partial x_i} = D_{ii}^* g_{ii} \tag{22}$$

$$D_{jj}^k = \frac{x_j D_{jj}^*}{RT} \cdot \frac{\partial \mu_j}{\partial x_j} = D_{jj}^* g_{jj} \tag{23}$$

$$D_{ki}^k = -\frac{D_{kk}^*}{RT}\left(x_i \frac{\partial \mu_i}{\partial x_i} + x_j \frac{\partial \mu_j}{\partial x_j}\right) = -D_{kk}^*(g_{ii} + x_j x_i g_{ji}) \tag{24}$$

$$D_{ij}^k = D_{ii}^k \left(\frac{\partial \mu_i / \partial x_j}{\partial \mu_i / \partial x_i}\right) = D_{ii}^k \frac{g_{ij}}{g_{ii}} \tag{25}$$

$$D_{ji}^k = D_{jj}^k \left(\frac{\partial \mu_j / \partial x_i}{\partial \mu_j / \partial x_j}\right) = D_{jj}^k \frac{g_{ji}}{g_{jj}} \tag{26}$$

$$D_{kj}^k = D_{ki}^k \left(\frac{\partial \mu_k / \partial x_j}{\partial \mu_k / \partial x_i}\right) = D_{ki}^k \frac{g_{kj}}{g_{ki}} \tag{27}$$

where D_{ii}^*, D_{jj}^*, and D_{kk}^* are referred to as the self-diffusion coefficients. Additionally, g_{ii}, g_{ij}, g_{ji}, and g_{kj} in the above equations represent the thermodynamic interaction coefficient. μ_i, μ_j, and μ_k are the chemical potentials. In order to calculate the interdiffusion coefficient D_{ii}, thermodynamic factors (g_{ii}, g_{ij}, g_{ji}, and g_{kj}) and self-diffusion coefficients (D_{ii}^*, D_{jj}^*, and D_{kk}^*) need to be obtained previously.

Based on the hard sphere theory of self-diffusion, Schwitzgebel [19] presented an approach to calculate the self-diffusion coefficients of components in liquid binary alloys. The self-diffusion coefficient of component i in the i-k binary alloy can be expressed as:

$$D_i^* = \frac{l_i}{2}\left(\frac{\pi RT}{M_i}\right)^{1/2} \frac{C(\delta)}{Z_x - 1} \tag{28}$$

where l_i is the atomic radius of component i, M_i is the mole mass of component i, $C(\delta)$ is the correction factor related to the packing fraction δ, and Z_x represents the compressibility factor. These parameters can be obtained in the literature [17,26].

The thermodynamic factor g, including g_{ii}, g_{ij}, g_{ji}, and g_{kj}, is defined by the equations below [27].

$$g_{ii} = \left(\frac{\partial \ln \alpha_i}{\partial \ln x_i}\right)_{x_j} = 1 + x_i \frac{\partial \ln \gamma_i}{\partial x_i} \tag{29}$$

$$g_{jj} = \left(\frac{\partial \ln \alpha_j}{\partial \ln x_j}\right)_{x_i} = 1 + x_j \frac{\partial \ln \gamma_j}{\partial x_j} \tag{30}$$

$$g_{ij} = \left(\frac{\partial \ln \alpha_i}{\partial \ln x_j}\right)_{x_i} = x_j \frac{\partial \ln \gamma_i}{\partial x_j} \tag{31}$$

$$g_{ji} = \left(\frac{\partial \ln \alpha_j}{\partial \ln x_i}\right)_{x_j} = x_i \frac{\partial \ln \gamma_j}{\partial x_i} \tag{32}$$

$$g_{ki} = \left(\frac{\partial \ln \alpha_k}{\partial \ln x_i}\right)_{x_j, x_k} = x_i \frac{\partial \ln \gamma_k}{\partial x_i} \tag{33}$$

$$g_{kj} = \left(\frac{\partial \ln \alpha_k}{\partial \ln x_j}\right)_{x_i, x_k} = x_j \frac{\partial \ln \gamma_k}{\partial x_j} \tag{34}$$

where α_i, α_j, and α_k are activities of three components in the ternary system. γ_i, γ_j, and γ_k represent activity coefficients of component i, j, and k, respectively. x_i, x_j, and x_k are mole fractions of three components in the ternary system.

3. Results and Discussion

3.1. Effect of Zr Addition on Thermodynamic Properties of Mg-Zn-Zr Alloys

3.1.1. Thermodynamic Properties of Mg-Zn, Mg-Zr, and Zn-Zr Alloys

Before predicting and studying the effect of Zr addition on thermodynamic properties of an Mg-Zn-Zr ternary system, it is necessary to learn the thermodynamic properties of the three constitutive binary systems of the Mg-Zn-Zr system. In this section, the mixing enthalpies and component activities of binary Mg-Zn, Mg-Zr, and Zn-Zr alloy systems are calculated according to the Miedema model (see Equations (1) and (3)). The calculation results are shown in Figure 1.

The mixing enthalpy is a thermodynamic parameter describing the strength of an interatomic interaction in liquid binary alloys. When the mixing enthalpy is negative in a binary alloy, it means that, unlike atoms that attract each other, they can form solid solutions and intermetallic compounds in the liquid of the binary alloy. Whereas the positive value of the mixing enthalpy means the unlikely atoms repel each other and, like atoms, tend to form clusters, which can result in a de-mixing tendency in the liquid binary alloy [28].
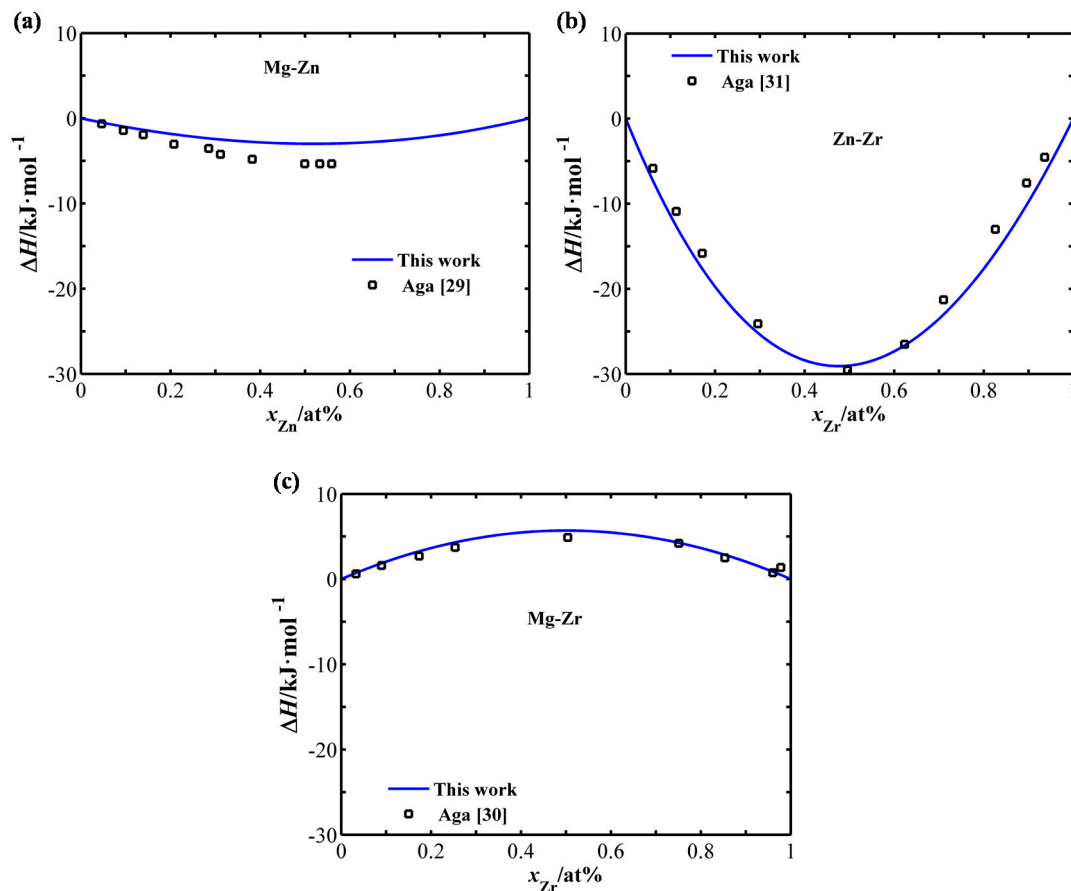

Figure 1. Calculated mixing enthalpy ΔH of liquid Mg-Zn (**a**), Zn-Zr (**b**), and Mg-Zr (**c**) alloys with experimental data and calculated Calphad-data from the literature [29–31].

In Figure 1, it is observed that the present calculated results are in good agreement with the available experimental data and calculated Calphad-data. The calculation of mixing enthalpy is at 0 K and the mixing enthalpy is independent of temperature in the Miedema model. This is one of the reasons that caused the small discrepancy between the calculation and experiment. The results of calculation are at 0 K but the experimental data were obtained at a nonzero temperature. In general, we can see that the present calculations for mixing enthalpy of binary alloys are reasonably correct.

As shown in Figure 1, the calculated mixing enthalpy of Mg-Zr alloys show a great difference from those of Mg-Zn and Zn-Zr alloys. The mixing enthalpies of Mg-Zn and Zn-Zr alloys are both negative over the whole composition range, while those of Mg-Zr alloys are positive. These results indicate that there is a repulsive interaction between Mg and Zr atoms, while the interactions between Mg and Zn atoms and between Zn and Zr atoms are both attractive. The result also indicates that compounds and solid solutions can be formed both in Mg-Zn and Zn-Zr binary systems while the Zr atoms prefer to form clusters with Zr atoms instead of combining with the Mg atoms in liquid Mg-Zr alloys. This means that there is a tendency for phase separation in the Mg-Zr system and that Zr atoms cannot combine with Mg to form stable compounds. According to the Mg-Zn and Zn-Zr phase diagrams (see Figure 2a,b), it can be found that many Mg-Zn and Zn-Zr compounds exist in Mg-Zn and Zn-Zr alloy systems, such as Mg_7Zn_3, $MgZn_2$, $MgZn$, Zn_2Zr, Zn_2Zr_3, $ZnZr_2$, and $ZnZr$ [32]. However, according to the Mg-Zr phase diagram (see Figure 2c), it can be found that the Mg-Zr intermetallic compound does not exist in the solid state. Besides, in the Mg-Zr phase diagram, we can also find that there is a de-mixing in the liquid state, which proves that there is actually a tendency for phase separation in the Mg-Zr system. Moreover, some experimental results can also support the prediction that Zr atoms prefer to form clusters with Zr atoms instead of combining with the Mg atoms in liquid Mg-Zr alloys. According to previous reports [33], the distribution of the soluble Zr in Zr-containing magnesium alloys is very inhomogeneous and almost all of the soluble zirconium is concentrated in zirconium-rich cores in the microstructure. In general, the calculated results have a good agreement with previous reports and phase diagrams.

In addition, according to Figure 1, it can also be found that the values of the mixing enthalpies of the Zn-Zr alloy are much more negative than those of the Mg-Zn alloy. It means that the attractive interaction between Zr and Zn atoms is much greater than that between Mg and Zn atoms. Zhang [34] pointed out that the more negative of the mixing enthalpy, the more likely the compounds can be formed in binary alloys. It can be concluded that the tendency to form compounds in Zn-Zr alloys is much greater than that in Mg-Zn alloys. The good agreements between the thermodynamic properties calculated by the Miedema model, the literature reports, and phase diagrams also prove the feasibility of the Miedema model in predicting the thermodynamic properties of Mg-Zn, Zn-Zr, and Mg-Zr alloys.
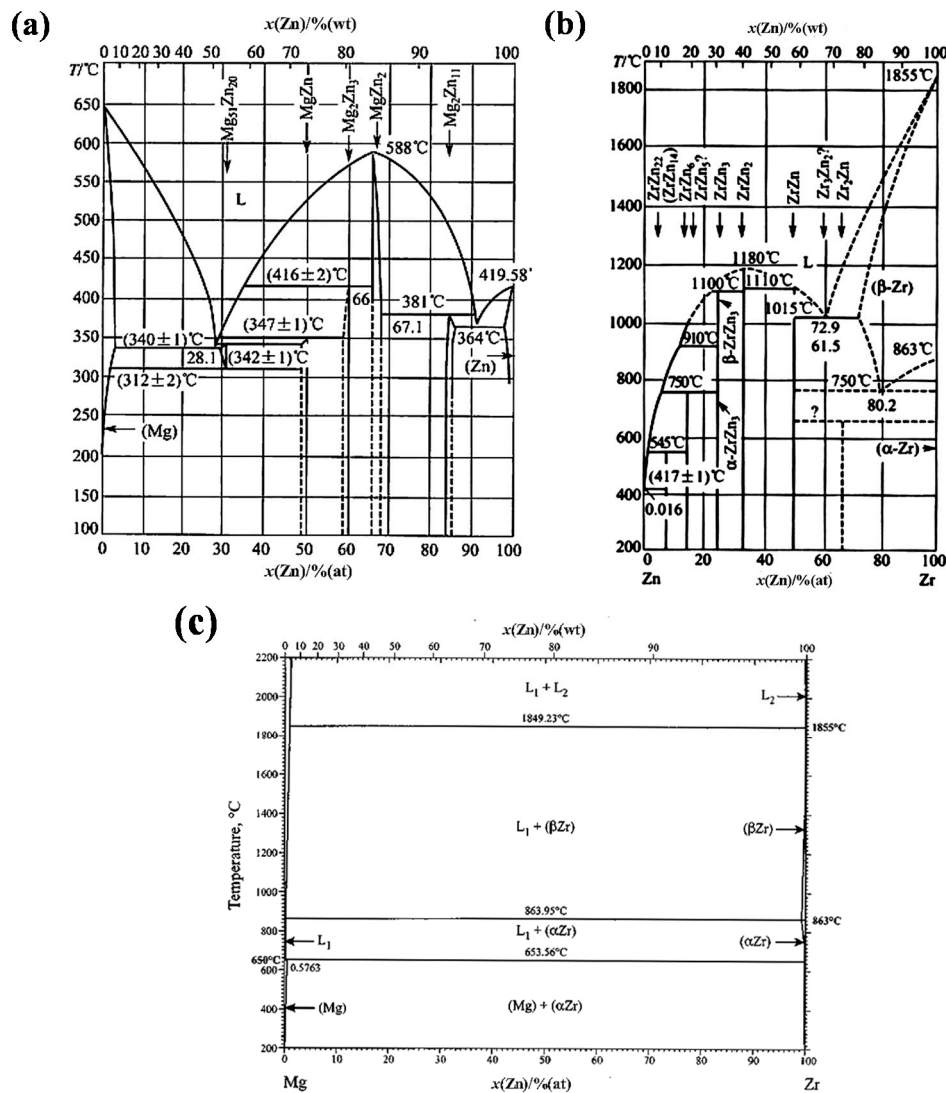
Figure 2. The Mg-Zn phase diagram (**a**), Zn-Zr phase diagram (**b**) adapted from [32], and the Mg-Zr phase diagram (**c**) adapted from [35], with permission from Springer, 2002.

The activities of components represent the effective compositions of these components in liquid alloys. According to Equation (16), the activity α_i of the component i can be expressed as $\alpha_i = \gamma_i \cdot x_i$, where γ_i is the activity coefficient and x_i is the mole fraction of component i. For an ideal melt ($\gamma = 1$), the activity of a component equals its mole fraction. The relationships in ideal melts between the component activities and compositions are shown in Figure 3. According to the deviation of components activity from the ideality, liquid binary alloys can be classified into two main types: negative deviation ($\gamma < 1$) or positive deviation ($\gamma > 1$). In liquid binary alloys, the more negative the deviation is, the greater the formation tendency of the compound is. In order to investigate the relationship between the formation tendency of the compound and temperature, the component activities of liquid Mg-Zn, Mg-Zr, and Zn-Zr binary alloys at different temperatures are calculated by Equations (16)–(18). According to the liquidus temperatures of Mg-Zn, Zn-Zr, and Mg-Zr binary phase diagrams (see Figure 2), the calculating temperatures of Mg-Zn alloys are selected in 960 K, 1000 K, and 1300 K and the calculating temperatures of Zn-Zr and Mg-Zr alloys are both selected in 2100 K, 2300 K, and 2500 K. The calculated curves of the component activities of liquid Mg-Zn, Zn-Zr, and Zn-Zr binary alloys at different temperatures are also shown in Figure 3.
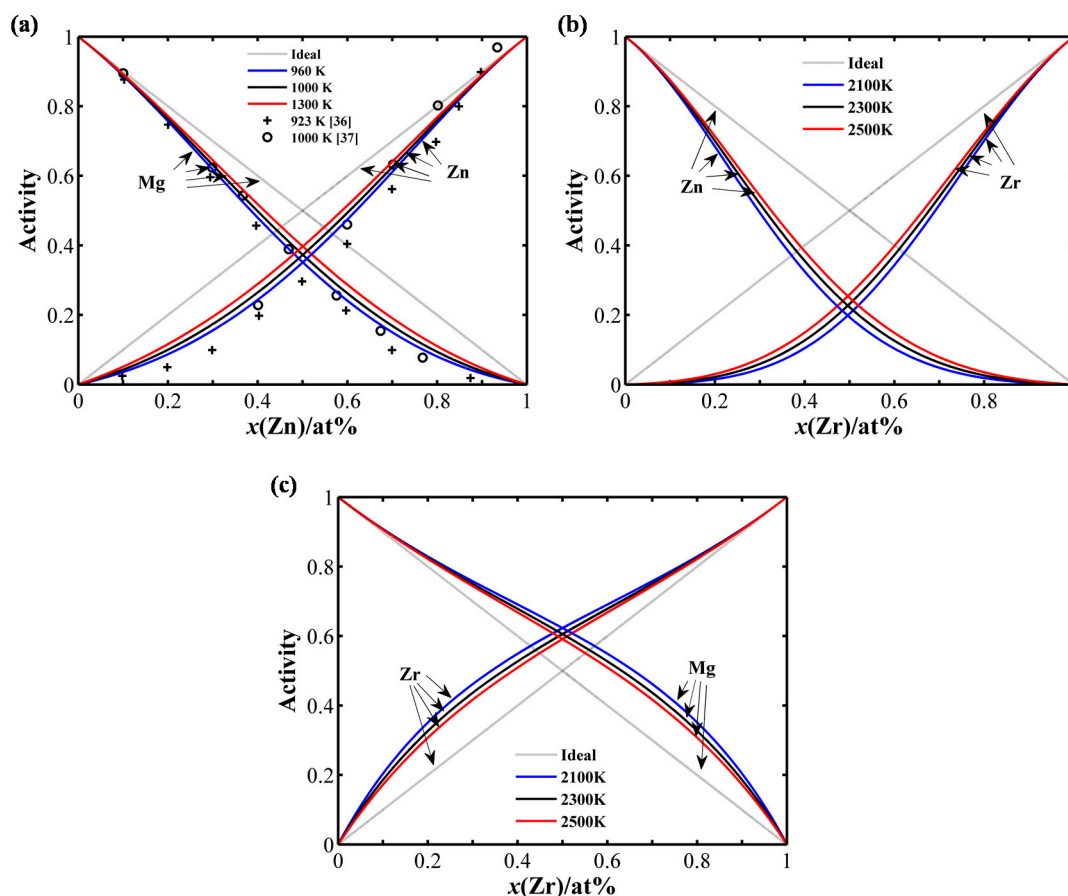
Figure 3. Calculated activities of the component of liquid Mg-Zn (**a**), Zn-Zr (**b**), and Mg-Zr (**c**) binary alloys with experimental data from the literature [36,37] at different temperatures.

From Figure 3a, the calculated activity values for Mg-Zn binary alloys have been compared with experimental values [36,37], and the present calculated results are in good agreement with the available experimental data in the Mg-Zn system. Because there are no experimental data available for liquid Zn-Zr and Mg-Zr alloys, a further comparison in Zn-Zr and Mg-Zr alloys cannot be performed.

In Figure 3a,b, it can be seen that the activity curves of the components of Mg-Zn and Zn-Zr alloys show negative deviations from those of idea melts. Yet, the activity curves of Mg-Zr alloys show positive deviations from their idea melts (see Figure 3c). These results imply that there is a repulsive interaction between Mg and Zr atoms, while the interactions between Mg and Zn atoms and between Zn and Zr atoms are both attractive. According to Figure 3a,b, with a decreasing temperature, the activity curves of Mg-Zn and Zn-Zr alloys both show greater negative deviations from their idea melts. That implies that the formation tendency of compounds become stronger with a decreasing temperature in Mg-Zn and Zn-Zr alloys. For Mg-Zr alloys (see Figure 3c), it can be found that the activity curves show a greater positive deviation from the ideal melt with a decreasing temperature. This indicates that the repulsive interaction between Mg and Zr atoms becomes stronger with a decreasing temperature, which will result in a more severe de-mixing in liquid Mg-Zr alloys with a decreasing temperature.

In sum, according to thermodynamic properties calculated by Miedema in this section, there is a repulsive interaction between Mg and Zr atoms in Mg-Zr alloys and the attractive interaction between Zr and Zn atoms is stronger than that between Mg and Zn atoms. The Mg-Zr intermetallic compound does not exist in Mg-Zr alloys while Mg-Zn and Zn-Zr compounds in Mg-Zn and Zn-Zr alloys can be formed. The thermodynamic properties calculated by the Miedema model have good agreement with

the literature reports and phase diagrams. It proves the feasibility of the Miedema model in predicting the thermodynamic properties of Mg-Zn, Zn-Zr, and Mg-Zr alloys.

As has been stated before, the formation enthalpies of Mg-Zn and Zn-Zr compounds can be obtained by Equations (2) and (3). Additionally, according to the literature [32], the melting temperatures of Mg-Zn and Zn-Zr compounds can be obtained. Therefore, the relationship between enthalpies of formation and melting temperatures of these compounds can be determined and shown in Figure 4. From Figure 4, it can be found that the compounds with more negative enthalpy of formation have higher melting temperatures. It is well known that a more negative enthalpy of formation is an indicator of a greater stability and stronger interatomic bonding [38]. At the same time, stronger bonding always leads to a higher melting temperature, which means that the relationship between calculated enthalpies of formation and melting temperatures, as shown in Figure 4, can further prove the accuracy of the calculation results. The higher melting temperatures and the more negative formation enthalpies of Zn-Zr intermetallics can cause the Zn-Zr intermetallic compounds instead of the Mg-Zn intermetallic compounds, which can take priority for depositing in the liquid Mg-6Zn-xZr (x = 0–6 wt%) alloys. The soluble Zn decreases, which is caused by intermetallic Zn–Zr particle formation in the melt. This can also result in the decrease in the amounts of Mg-Zn compounds.
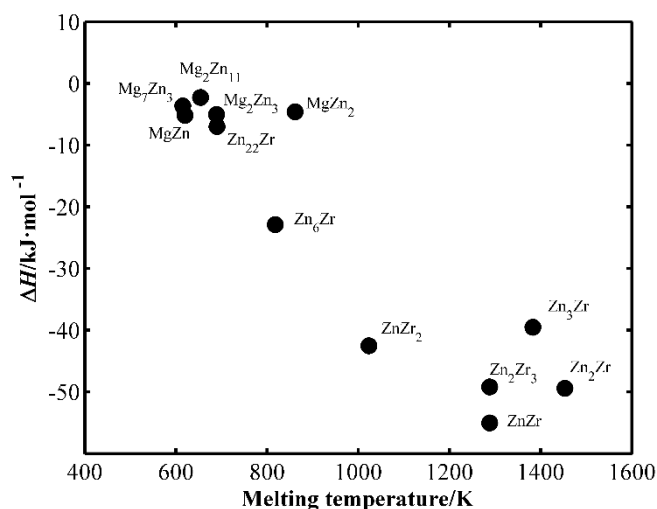

Figure 4. Relationship between enthalpies of formation and melting temperature [32] of some binary inter-metallics.

Lastly, from the above calculation results of binary alloys (see part 1 of Section 3.1), it can be found that the Mg-Zr intermetallic compound does not exist and only Mg-Zn and Zn-Zr intermetallic compounds exist in the Mg-6Zn-xZr (x = 0–0.6 wt%) alloys. At the same time, some experimental results reported in the literature prove that the main strengthening phase are Mg_7Zn_3, $MgZn_2$, and $MgZn$ in Mg-6Zn-xZr (x = 0–6 wt%) alloys [7,8]. Therefore, it can be concluded that research should be the focus on the effect of Zr addition on the formation of Mg-Zn compounds in the Mg-6Zn-xZr (x = 0–0.6 wt%) alloys. That is the reason why only the Gibbs free energy associated with the formation of Mg-Zn compounds are calculated according to Equations (13)–(15) in this paper.

3.1.2. Effect of Zr Addition on Thermodynamic Properties of Mg-6Zn-xZr (x = 0–6 wt%) Alloys

In this section, based on the above calculation results of constitutive binary systems, thermodynamic properties of the Mg-Zn-Zr ternary alloys are calculated by the Chou model. According to the calculation results, the effects of Zr addition on the thermodynamic properties in liquid Mg-Zn-Zr alloys and the precipitation behaviors of Mg-Zn and Zn-Zr compounds are discussed in Mg-6Zn-xZr (x = 0–0.6 wt%).

Among the thermodynamic properties of Mg-Zn-Zr alloys, the mixing enthalpies over the whole composition range are calculated by Equations (5)–(9). The composition dependencies of the mixing enthalpies of the liquid Mg-Zn-Zr ternary alloys are illustrated in Figure 5a. To make a more explicit description for the thermodynamic parameters, the curved surfaces in Figure 5a are projected onto a plane and then the rectangular coordinate system is converted into a triangular coordinate system (see Figure 5b). It can be seen that the mixing enthalpies of the Mg-Zn-Zr ternary alloys are positive in the region for low zinc concentration (see the region B in Figure 5b). On the contrary, the mixing enthalpies of liquid Mg-Zn binary alloys are all negative over the whole composition range (see Figure 1). The reason rises from the repulsive interaction between Mg and Zr, which has been discussed in the above statements about the interactions between atoms (see part 1 of Section 3.1). Additionally, it can be seen from Figure 5b that the minimum values of ΔH is obtained at the point A ($x_{Zn} = 52.4\%$, $x_{Zr} = 47.6\%$, $x_{Mg} = 0\%$), which is located at the Zn-Zr edge of the composition triangle. This result indicates that there is still a strong attractive interaction between Zn and Zr in Mg-Zn-Zr alloys. Lastly, according to Figure 5b, the mixing enthalpy ΔH of the Mg-6Zn-xZr ($x = 0\sim0.6$ wt%) alloys can be found to be negative. According to the calculation results by the Miedema model, the values of ΔH increase from -0.29 kJ/mol for the Mg-6 wt% Zn-0 wt% Zr alloy to -0.26 kJ/mol for the Mg-6 wt% Zn-0.6 wt% Zr alloy. Therefore, the addition of Zr elements into the Mg-6 wt% Zn alloy can increase the mixing enthalpy.
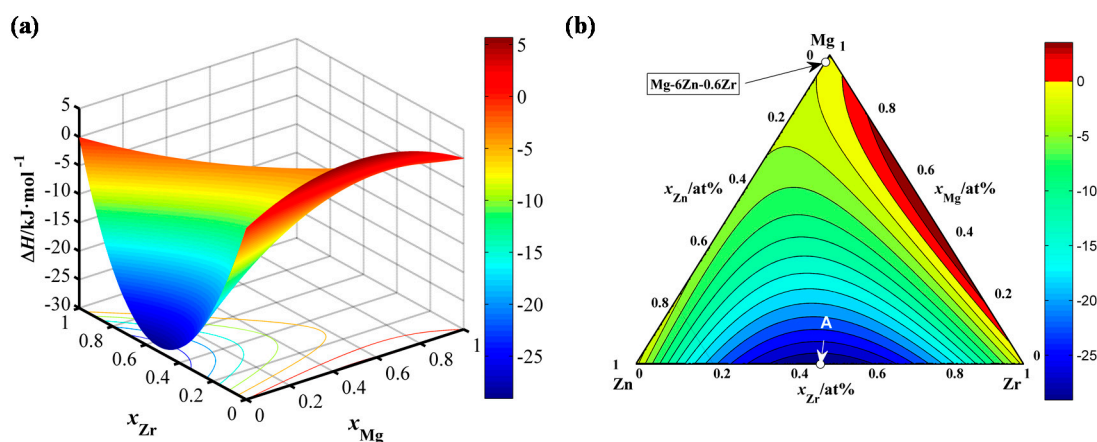

Figure 5. Three-dimensional diagram (**a**) and isogram (**b**) of the mixing enthalpy of liquid Mg-Zn-Zr alloys.

The addition of Zr can influence the Gibbs free energy of formation of Mg-Zn compounds by changing the component activities in Mg-6Zn-xZr ($x = 0$–6 wt%) and, consequently, influence the nucleation of these strengthening phases. Therefore, in order to further investigate the effect of Zr addition on the precipitation properties of Mg-Zn compounds, it needs to calculate the activity changes of Zn and Mg caused by Zr addition in liquid Mg-6Zn-xZr ($x = 0$–6 wt%) alloys.

The activity coefficients of Mg and Zn at different temperatures in the liquid Mg-6Zn-xZr ($x = 0$–0.6 wt%) alloys are calculated by Equations (16)–(20). Because the melting temperature of Mg-6Zn-xZr ($x = 0$–0.6 wt%) alloys are below 950 K [39], the researched temperatures are selected at 950 K, 1050 K, and 1159 K. The calculation results about activity coefficients of Mg and Zn are shown in Figure 6, which can clearly show the relationships between the mass fraction of the Zr component and the activity coefficients of components in the liquid Mg-6Zn-xZr ($x = 0$–0.6 wt%) alloys.
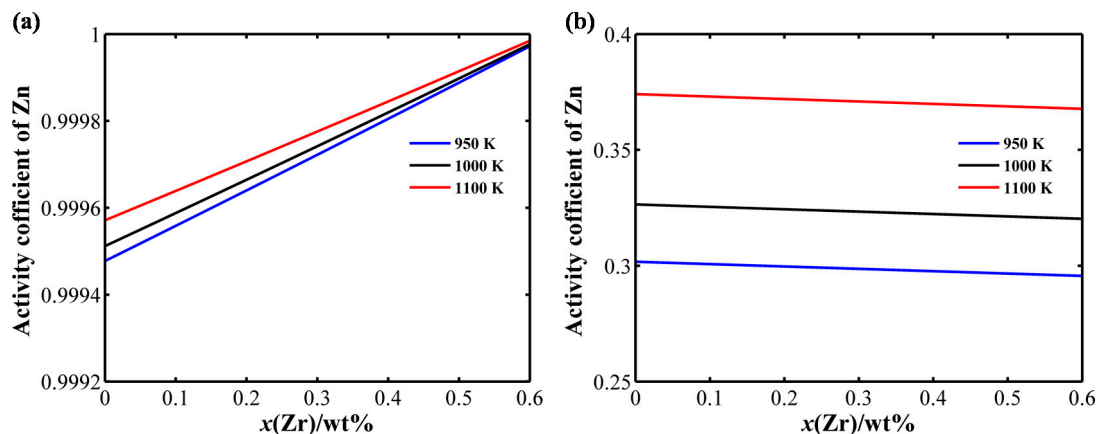
(a)

(b)

Figure 6. Effect of Zr addition on the activity coefficients of Mg and Zn in Mg-6Zn-*x*Zr melts at different temperatures, (**a**) Mg; (**b**) Zn.

The activities of components represent the actual effective compositions of these components in liquid alloys, which is related to the precipitation of atoms in liquid alloys. Therefore, based on the deviation of the component activity between the actual mixture from the ideal mixture, the precipitation properties of atoms can be predicted.

First, it can be seen from Figure 6 that the activity coefficients of Mg and Zn in Mg-6Zn-*x*Zr (*x* = 0–0.6 wt%) alloys are all below 1, which means the activities of Mg and Zn both show negative deviations from ideality. It also implies that Mg and Zn can both precipitate in their ternary alloys. According to the former discussion, these compounds are mainly the Mg-Zn and Zn-Zr intermetallic compounds. Since the attractive interaction between Zr and Zn atoms is stronger than that between Mg and Zn atoms (see part 1 of Section 3.1), Zr atoms tend to combine Zn atoms rather than Mg atoms. Therefore, the Zn-Zr intermetallic compounds, not the Mg-Zn intermetallic compounds, can take priority of depositing in the liquid Mg-6Zn-*x*Zr alloys. Secondly, Figure 6 show that the activity coefficient of Mg is very close to 1 in their ternary alloys (see Figure 6a) while the activity coefficient of Zn is much smaller than 1 (see Figure 6b). Those results mean that the activity of Mg shows a very small negative deviation from ideality while the activity of Zn shows a large negative deviation from ideality. It can be concluded that the majority of Zn exists in the form of intermetallic compounds in the Mg-6Zn-*x*Zr alloys. Third, it can be seen from Figure 6 that the activity coefficients of Mg and Zn both grow as the temperature increases, which means that their negative deviations of activity from ideality both reduce with increasing the temperature. Therefore, it can be concluded that the decreasing temperature can promote the precipitation phases (e.g., the Mg-Zn and Zn-Zr intermetallic compounds). Lastly, Figure 6 show that the activity coefficients of Mg increases with increasing Zr content, while the activity coefficient of Zr reduces with increasing Zr content. For the activity of Mg, the negative deviation from ideality should reduce with increasing Zr content, and, for the activity of Zr, the negative deviation from ideality should become greater with increasing Zr content. The result means that the addition of Zr can hinder the precipitation of Mg atoms and promote the precipitation of Zn atoms. In order to discuss the effect of Zr addition on the precipitation of Mg-Zn compounds, the two different effects of Zr on Mg and Zn atoms need to be considered together. Therefore, the Gibbs free energies of Mg-Zn compounds, which are decided by the activities of Mg and Zn in the meantime, need to be obtained.

In order to accurately describe the effect of Zr addition on the precipitation property of Mg-Zn compounds, the Gibbs free energies of Mg-Zn compounds need to be calculated. The calculation for Gibbs free energies (ΔG) of Mg-Zn compounds is carried out according to Equations (10)–(15). Figure 7 shows the calculated curves of the changes of ΔG of Mg_7Zn_3, $MgZn_2$, and $MgZn$ with increasing Zr content at 950 K, 1050 K, and 1159 K.

According to Figure 7, it can be found that the change of ΔG of Mg_7Zn_3, $MgZn_2$, and MgZn are all positive and increase with increasing Zr content. These results indicate that the addition of Zr addition increase Gibbs free energies of formation of Mg_7Zn_3, $MgZn_2$, and MgZn, from which it can be concluded that the addition of Zr hinders the formation of Mg_7Zn_3, $MgZn_2$, and MgZn. This hindering effect becomes stronger with increasing Zr content. Moreover, the change of Gibbs free energies of Mg_7Zn_3, $MgZn_2$, and MgZn all become greater with decreasing temperature, which indicates that the hindering effect of Zr addition on the formation of Mg_7Zn_3, $MgZn_2$, and MgZn become stronger with higher temperatures.
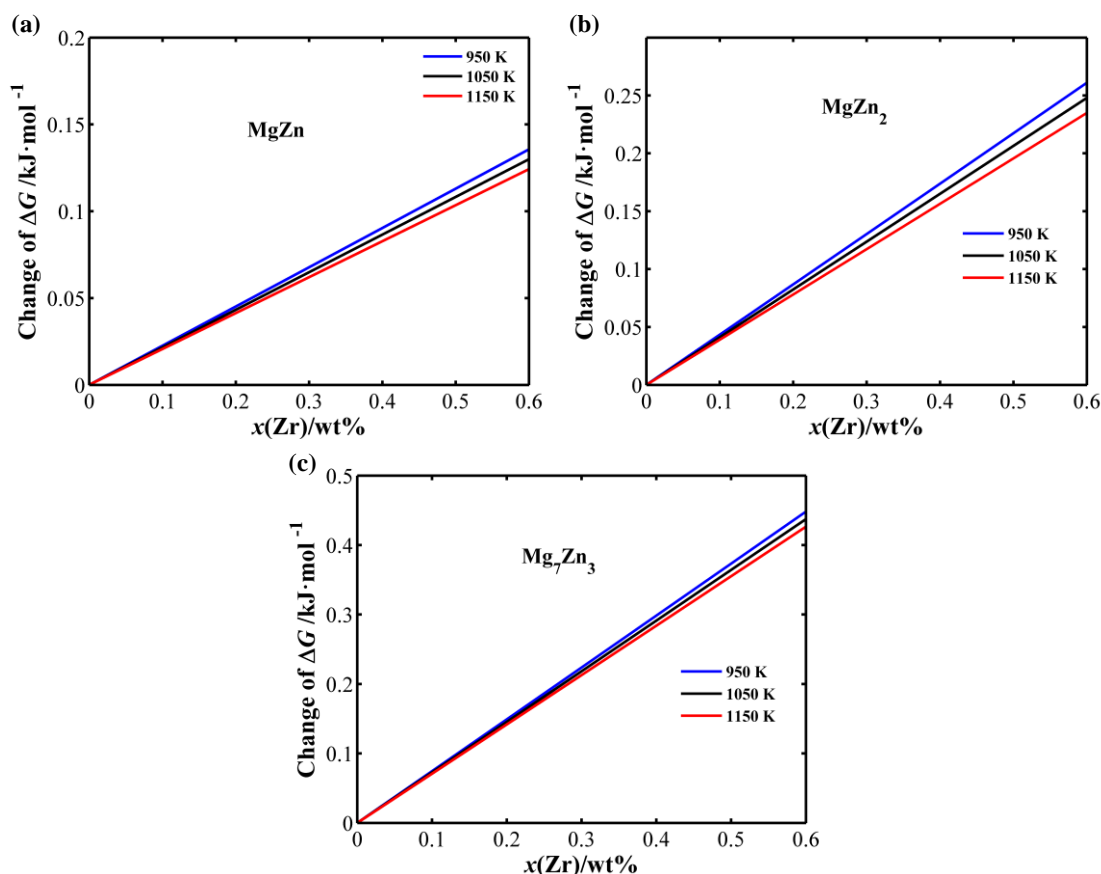

Figure 7. Effect of Zr addition on the change of ΔG associated with formation of Mg-Zn compounds in Mg-6Zn-xZr (x = 0–0.6 wt%) melts at different temperatures, (**a**) MgZn; (**b**) $MgZn_2$; (**c**) Mg_7Zn_3.

3.2. The Effects of Zr and Zn Additions on Kinetic Properties of Elements

Previously, the effects of Zr addition on the thermodynamic properties of Mg-6Zn-xZr alloys have been discussed. However, such thermodynamic investigations cannot predict the formation kinetics of Mg-Zn compounds. The addition of Zr can influence the diffusion rates of Zn and Zr by changing the interdiffusion coefficients in the Mg-6Zn-xZr (x = 0–6 wt%) melt, and, consequently, influence the growth of Mg-Zn compounds. In this paper, the interdiffusion coefficients of the solute components in ternary Mg-Zn-Zr alloys are calculated first, and then the influence of Zr addition on the diffusion of the solute components is discussed in Mg-6Zn-xZr (x = 0–0.6 wt%) alloys. Additionally, in order to investigate the effect of Zn addition on the diffusion of the solute components, the Zn content is fixed at 6 wt% and the Zn content varies from 0 wt% to 6 wt% first and then the diffusion coefficients in liquid Mg-xZn-0.6Zr (x = 0–6 wt%) alloys are calculated.

The four ternary interdiffusion coefficients (D_{ZnZn}, D_{ZrZr}, D_{ZnZr}, and D_{ZrZn}) of Mg-Zn-Zr ternary alloys can be calculated by Equations (14)–(28). D_{ZnZn} and D_{ZrZr} are the main coefficients of Zn and Zr atoms in Mg-Zn-Zr ternary alloys, respectively. The main interdiffusion coefficients (D_{ZnZn}, D_{ZrZr})

represent the influence of the concentration gradient of a component on its own fluxes. Namely, the main interdiffusion coefficients D_{ZnZn} and D_{ZrZr} depend on the composition of Zn and Zr, respectively. D_{ZnZr} and D_{ZrZn} are the cross interdiffusion coefficients of Zn and Zr atoms in Mg-Zn-Zr ternary alloys, respectively. The cross interdiffusion coefficients (D_{ZnZr}, D_{ZrZn}) represent the influence of the concentration gradient of a component on the flux of the other component. Namely, the cross interdiffusion coefficient D_{ZnZr} of Zn depends on the composition of Zr while the cross interdiffusion coefficient D_{ZrZn} of Zr depends on the composition of Zn.

According to the above definitions, the Zr composition can influence the main interdiffusion coefficients (D_{ZrZr}) of Zr atoms and the cross interdiffusion coefficients (D_{ZnZr}) of Zn atoms. As shown in Figure 8, the absolute value of the cross interdiffusion coefficient D_{ZnZr} of Zn atoms decrease with increasing Zr concentration up to 0.6 wt.%, while the absolute value of the main interdiffusion coefficient D_{ZrZr} of Zr atoms slightly decreases and is almost constant with increasing Zr concentration up to 0.6 wt%. This result shows that the addition of Zr can hinder the diffusion of Zn and have little influence on the diffusion of Zr in liquid Mg-6Zn-xZr (x = 0~0.6 wt%) alloys. It is known that alloy addition can influence the diffusion coefficients of solute components and, hence, influence the grain growth rate of compounds [40]. Moreover, the grain sizes of Mg-Zn compounds (Mg_7Zn_3, $MgZn_2$, and MgZn) depend on the diffusion rate of the solute Zn in Mg-6Zn-xZr alloys. Therefore, the calculated result means the addition of Zr can hinder the grain growth of Mg-Zn compounds and, consequently, lead to smaller grain sizes of Mg-Zn compounds (Mg_7Zn_3, $MgZn_2$, and MgZn). According to the experimental results reported in the literature [7], the addition of Zr can reduce the size of the Mg-Zn compounds. Clearly, the calculation results in this paper have excellent agreement with the experimental results.
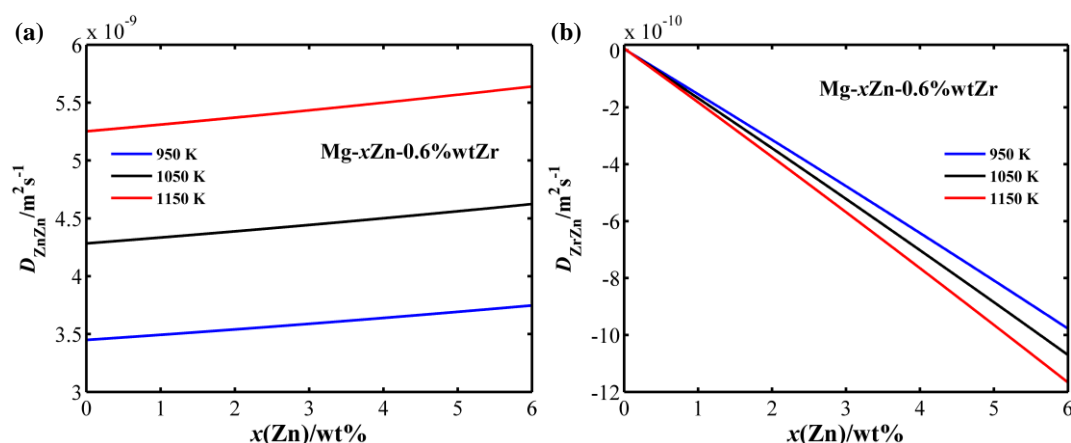

Figure 8. Dependence of the main interdiffusion coefficient D_{ZrZr} (**a**) of Zr atoms and the cross interdiffusion coefficient D_{ZnZr} (**b**) of Zn atoms on the composition of Zr in the liquid Mg-6 wt% Zn-xZr alloys at 950 K, 1050 K, and 1150 K.

Analogously, according to the above definitions, the Zn composition can only influence the main interdiffusion coefficients (D_{ZnZn}) of Zn and the cross interdiffusion coefficient (D_{ZrZn}) of Zr. From Figure 9, it can be seen that the absolute values of the main interdiffusion coefficient (D_{ZnZn}) of Zn and the cross interdiffusion coefficient (D_{ZrZn}) of Zr increase with increasing Zn concentration up to 6wt% in the liquid Mg-xZn-0.6Zr (x = 0–6 wt%) alloys. These results indicate that the increase of Zn content can promote the diffusion of Zn and Zr in the liquid Mg-xZn-0.6Zr (x = 0–6 wt%) alloys, and, consequently, promote the growth of Mg-Zn compounds.
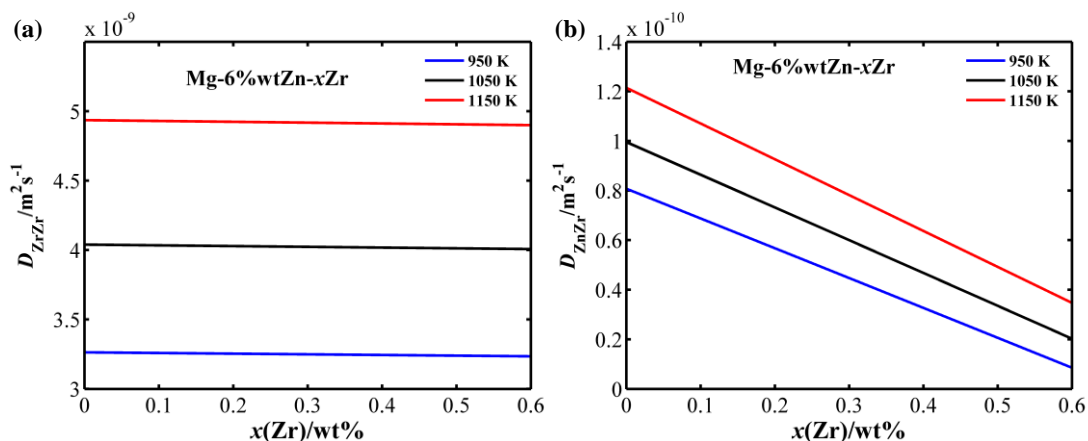
Figure 9. Dependence of the main interdiffusion coefficient D_{ZnZn} (**a**) of Zn atoms and the cross interdiffusion coefficient D_{ZrZn} (**b**) of Zr atoms on the composition of Zn in the liquid Mg-*x*Zn-0.6 wt% Zr alloys at 950 K, 1050 K, and 1150 K.

Lastly, Figures 8 and 9 also show that the cross interdiffusion coefficients are about one order of magnitude smaller than the main interdiffusion coefficients. Since the absolute values of these four interdiffusion coefficients all increase with increasing temperature, the component Zn and Zr diffuse faster in the liquid Mg-Zn-Zr alloys at higher temperatures, which will influence the formation of precipitated compounds.

4. Conclusions

In this paper, the effect of Zr addition on the thermodynamic and kinetic properties of the Mg-6Zn-*x*Zr (*x* = 0–6 wt%) alloys are calculated and evaluated by using the Miedema model, the Chou model, and the diffusion predicting model. At the same time, the effect of Zr addition on the precipitation properties of compounds in Mg-6Zn-*x*Zr (*x* = 0–6 wt%) are also discussed according to the calculation results.

(1) The calculation results about mixing enthalpies of liquid Mg-Zn, Mg-Zr, and Zn-Zr alloys shows that the interaction between Mg and Zr atoms is repulsive, while the interactions between Mg and Zn atoms and between Zn and Zr atoms are both attractive. The attractive interaction between Zn and Zr atoms is stronger than that between Mg and Zn atoms. These results can explain why Mg cannot combine with Zr to form stable compounds, while Mg can combine with Zn and Zn can combine with Zr to form stable compounds. The calculated thermodynamic properties by the Miedema model have good agreement with previous reports and corresponding phase diagrams.

(2) The component activity of liquid Mg-Zn, Mg-Zr, and Zn-Zr alloys predicted at different temperatures show that the tendency for compound formation become greater with decreasing temperature in the Mg-Zn and Zn-Zr alloys. The predicted results also indicate that the repulsive interaction between Mg and Zr atoms become stronger with a decreasing temperature.

(3) Compared with the mixing enthalpy of the liquid Mg-6Zn binary alloys, the Zr addition decreases the mixing enthalpy of Mg-6Zn-*x*Zr (*x* = 0–6 wt%) alloys. At the same time, the Zr addition will increase the activity of Mg and decrease the activity of Zr. This result will lead to the Gibbs free energy changes of Mg_7Zn_3, $MgZn_2$, and MgZn are positive and increase with increasing Zr content, which indicates that the Zr addition can hinder the formation of Mg_7Zn_3, $MgZn_2$, and MgZn compounds thermodynamically. The hindering effect of Zr addition on the formation of Mg_7Zn_3, $MgZn_2$, and MgZn become stronger at a higher temperature.

(4) The calculated main and cross interdiffusion coefficients of Zn and Zr in ternary Mg-Zn-Zr alloys show that the increase of Zn content can promote the diffusion of Zn and Zr while the increase of Zr content can suppress the diffusion of Zn and Zr in liquid Mg-Zn-Zr alloys. In other words, Zr can

hinder the growth of Mg-Zn compounds in Mg-6Zn-xZr (x = 0–6 wt%) alloys. Lastly, the component Zn and Zr diffuse faster with higher temperatures in liquid Mg-Zn-Zr alloys.

Author Contributions: Conceptualization, Y.Y. and Y.H. Methodology, Y.Y. and Y.H. Software, Y.Y. Validation, Y.Y. Formal analysis, Y.Y. Investigation, Y.Y. and Y.H. Resources, Y.H. and Q.W. Data curation, Y.Y. Writing—original draft preparation, Y.Y. Writing—review and editing, Y.H. Visualization, Y.Y. Supervision, Y.H. and Q.W. Project administration, Y.H. and Q.W. Funding acquisition, Y.H. and Q.W.

References

1. Kulekci, M.K. Magnesium and its alloys applications in automotive industry. *Int. J. Adv. Manuf. Tech.* **2008**, *39*, 851–865. [CrossRef]

2. Mordike, B.L.; Ebert, T. Magnesium: Properties-applications-potential. *Sci. Eng. A* **2001**, *302*, 37–45. [CrossRef]

3. Mordike, B.L. Development of highly creep resistant magnesium alloys. *Mater. Sci. Eng. A* **2001**, *117*, 391–394. [CrossRef]

4. Ali, Y.; Qiu, D.; Jiang, B.; Pan, F.; Zhang, M.X. Current research progress in grain refinement of cast magnesium alloy. *J. Alloys Compd.* **2015**, *619*, 639–651. [CrossRef]

5. Singh, A.; Tsai, A.P. Structural characteristics of β1' precipitates in Mg-Zn-based alloys. *Scr. Mater.* **2007**, *57*, 941–944. [CrossRef]

6. Lee, Y.C.; Dahle, A.K.; StJohn, D.H. The role of solute in grain refinement of magnesium. *Metall. Mater. Trans. A* **2000**, *31*, 2895. [CrossRef]

7. Hildebrand, Z.C.; Qian, M.; StJohn, D.H.; Frost, M.T. Influence of zinc on the soluble zirconium content in magnesium and the subsequent grain refinement by zirconium. In Proceedings of the 133rd Annual Meeting and Exhibition (TMS 2004), Warrendale, PA, USA, 14–18 March 2004; pp. 241–245.

8. Ma, Y.L.; Pan, F.S.; Zuo, R.L.; Zhang, J.; Yang, M.B. The Influence of Zinc and Zirconium on the Microstructure of the As-Cast Magnesium Alloy ZK60. *Mater. Sci. Forum* **2007**, *546*, 369–372. [CrossRef]

9. Zhang, X.; Zhang, Y.N.; Kevorkov, D.; Medraj, M. Experimental investigation of the MgZnZr ternary system at 450 °C. *J. Alloys Compd.* **2016**, *680*, 212–225. [CrossRef]

10. Kirkaldy, J.S. Diffusion in multicomponent metallic systems: ii. solutions for two-phase systems with applications to transformations in steel. *Can. J. Phys.* **1958**, *3*, 907–916. [CrossRef]

11. Servi, I.S.; Turnbull, D. Thermodynamics and kinetics of precipitation in the copper-cobalt system. *Acta Metall.* **1966**, *14*, 161–169. [CrossRef]

12. De Boer, F.R.; Mattens, W.C.M.; Boom, R.; Miedema, A.R.; Niessen, A.K. *Cohesion in Metals: Transition Metal Alloys*; Elsevier Science Publishers, B.V.: Amsterdam, The Netherlands, 1988; pp. 20–65, ISBN 0444870989.

13. Chou, K.C. A General Solution Model for Predicting Ternary Thermodynamic Properties. *Calphad* **1995**, *19*, 315–325. [CrossRef]

14. Chou, K.C.; Wei, S.K. A new generation solution model for predicting thermodynamic properties of a multicomponent system from binaries. *Metall. Mater. Trans. B* **1997**, *28*, 439–445. [CrossRef]

15. Zhang, G.H.; Chou, K.C. General formalism for new generation geometrical model: Application to the thermodynamics of liquid mixtures. *J. Solut. Chem.* **2010**, *3*, 1200–1212. [CrossRef]

16. Kirkaldy, J.S.; Young, D.J. *Diffusion in the Condensed State*; The Institute of Metals: London, UK, 1987; pp. 161–165, ISBN 0-0-43557-87-2.

17. Protopapas, P.; Andersen, H.C.; Parlee, N.A.D. Theory of transport in liquid metals. I. Calculation of self-diffusion coefficients. *J. Chem. Phys.* **1973**, *59*, 15–25. [CrossRef]

18. Ding, X.; Chen, X.; Rogl, P.; Morral, J.E. Prediction Model of Diffusion Coefficients for Ternary Alloy. *Acta Metall. Sin.* **2000**, *36*, 823–827.

19. Schwitzgebel, G.; Langen, G. Application of the hard sphere theory to the diffusion of binary liquid alloy systems. *Z. Naturforsch. A* **1981**, *36*, 1225–1232. [CrossRef]

20. Jin, L.; Kevorkov, D.; Medraj, M.; Chartrand, P. Al–Mg–RE (RE = La, Ce, Pr, Nd, Sm) systems: Thermodynamic evaluations and optimizations coupled with key experiments and Miedema's model estimations. *J. Chem. Thermodyn.* **2013**, *58*, 166–195. [CrossRef]

21. Tanaka, T.; Gokcen, N.A.; Morita, Z.I.; Lida, T. Thermodynamic relationship between enthalpy of mixing and excess entropy in liquid binary alloys. *Z. Metallkd.* **1993**, *84*, 192–199.

22. Ouyang, Y.; Zhong, X.; Du, Y.; Jin, Z.; He, Y.; Yuan, Z. Formation enthalpies of Fe–Al–RE ternary alloys calculated with a geometric model and Miedema theory. *J. Alloys Compd.* **2006**, *416*, 148–154. [CrossRef]

23. Ren, Y.P.; Guo, Y.; Chen, D.; Li, S.; Pei, W.L.; Qin, G.W. Isothermal section of Mg–Zn–Zr ternary system at 345 °C. *Calphad* **2011**, *35*, 411–415. [CrossRef]

24. Da-Lun, Y.E.; Jianhua, H. *Thermodynamic Data Handbook of Inorganic Material*; Metallurgical Industry Press: Beijing, China, 2004; pp. 6–26, ISBN 978-75-0243-055-9.

25. Xueyong, D.; Peng, F.A.N.; Qiyong, H. Models of Activity and Activity Interaction Parameter in Ternary Metallic Melt. *Acta Metall. Sin.* **1994**, *30*, 49–60.

26. Crawley, A.F. Densities of liquid metals and alloys. *Int. Metall. Rev.* **1974**, *19*, 32–48. [CrossRef]

27. Živković, D.; Živković, Ž.; Liu, Y.H. Comparative study of thermodynamic predicting methods applied to the Pb–Zn–Ag system. *J. Alloys Compd.* **1998**, *265*, 176–184. [CrossRef]

28. Ponec, V. Alloy catalysts: The concepts. *Appl. Catal. A* **2001**, *222*, 31–45. [CrossRef]

29. Agarwal, R.; Sommer, F. Calorimetric investigations of Mg–Zn and Mg–Y liquid alloys. In Proceedings of the 8th National Symposium Thermal Analysis, Bombay, India, 10–11 January 1991; p. 249.

30. Arroyave, R.; Shin, D.; Liu, Z.K. Modification of the thermodynamic model for the Mg–Zr system. *Calphad* **2005**, 230–238. [CrossRef]

31. Arroyave, R.; Liu, Z.K. Thermodynamic modelling of the Zn–Zr system. *Calphad* **2006**, 1–13. [CrossRef]

32. Лякишев, Н.П. *Handbook of Metal Binary Phase Diagram*; Chemical Industry Press: Beijing, China, 2008; pp. 914–916, ISBN 9787122027047.

33. Qian, M.; StJohn, D.H.; Frost, M.T. Characteristic zirconium-rich coring structures in Mg–Zr alloys. *Scr. Mater.* **2002**, *46*, 649–654. [CrossRef]

34. Zhang, Y.; Zhou, Y.J.; Lin, J.P.; Chen, G.L.; Liaw, P.K. Solid-solution phase formation rules for multi-component alloys. *Adv. Eng. Mater.* **2008**, *10*, 534–538. [CrossRef]

35. Okamoto, H. Mg-Zr (magnesium-zirconium). *J. Phase Equilib.* **2002**, *23*, 198–199. [CrossRef]

36. Moser, Z. Thermodynamic properties of dilute solutions of magnesium in zinc. *Metall. Trans.* **1974**, *5*, 1445–1450. [CrossRef]

37. Chiotti, P.; Stevens, E.R. Thermodynamic Properties of Magnesium-Zinc Alloys. *Trans. Metall. Soc. AIME* **1965**, *233*, 198.

38. Duan, Y.H.; Sun, Y.; Lu, L. Thermodynamic properties and thermal conductivities of $TiAl_3$-type intermetallics in Al–Pt–Ti system. *Comput. Mater. Sci.* **2013**, *68*, 229–233. [CrossRef]

39. Bhan, S.; Lal, A. The Mg-Zn-Zr system (magnesium-zinc-zirconium). *J. Phase Equilib.* **1993**, *14*, 634–637. [CrossRef]

40. Zhang, C.; Fan, T.; Cao, W.; Ding, J. Size control of in situ formed reinforcement in metal melts-theoretical treatment and application to in situ (AlN + Mg_2Si)/Mg composites. *Compos. Sci. Technol.* **2009**, *69*, 2688–2694. [CrossRef]